Synthesis a New Series of Methenamine Complexes with Some Different Metal Ions: Spectral, Thermal and Biological Investigations

Soha F. Mohammed[1*,] Moamen S. Refat [2,3] and Nashwa M. El – Metwaly [4,5]

1[*]Chemistry Department, Faculty of Science, Zagazig University, Zagazig Egypt
[2]Chemistry Department, Faculty of Science, Port Said University, Port Said, Egypt
[3]Chemistry Department, Faculty of Science, Taif University, 888 Taif, Saudi Arabia
[4]Chemistry Department, Faculty of Education of Girls, King Khaled University, Saudi Arabia
[5]Chemistry Department, Faculty of Science, Mansoura University, Egypt
sofahim@yahoo.com

Abstract: In this paper methenamine (HMTA) ligand acts as monodentate with each central atom in all isolated complexes although the ligand molecule possesses four potential donor atoms through three fused rings in the chair configuration with four bridges – head nitrogen atoms. The nitrogen atoms of this donor may permeate the coordination towards multinucleous of metal atoms. This behavior may be due to the shape of the ligand distribute the donor atoms by the shape leads to this coordination. Ag(I), Cd(II), Cu(II), Hg(II), Sn(II), Sn(IV), Sb(III), Bi(III), Ce(III), Sm(III) and La(III) are the metal ions concerned this study. In the infrared spectra the shift in υ(C-N) bands proposed the type of coordination mode. The ^{1}HNMR spectra of Sn(II) and Bi(III) complexes are further supported for the proposed chelation. The XRD study for some selective complexes reflects their amorphous nature. The thermal behavior of these chelates shows that the hydrated complexes losses water molecules of hydration and coordination at relatively higher temperature. This is due to the presence of hydrated molecules introduced by H – bonding inside the coordination sphere with the active ligand centers followed immediately by decomposition of anions and ligand molecules in the subsequent steps. The activation thermodynamic parameters as; E*, ΔH*, ΔS* and ΔG* are calculated from the TG curves using Coats – Redfern method for suitable TG curves in between the all, which display peaks in between sharpness and broadness. The ligand in comparison to some of complexes was screened for their antibacterial and antifungal activities. The application was concerned in this study with focusing on some special complexes chosen referring to their history of their distinguish activity. The activity data show the investigated metal complexes to be more potent than the parent organic against most species.

1. Introduction

Crystal engineering and the design of solid-state architectures of coordination polymer are very attractive fields in literatures , due to their potential applications in catalysis, separations and optoelectronics [1-6]. Assembly of such extended supramolecular architectures by selecting the coordination geometry of metal ions and the chemical structure property of organic ligands can give rise to new and varied topological types [7–24]. Methenamine (HMTA), a potential tetradentate ligand, has been used to assemble new supramolecular architectures with metal ions via various possible coordination modes, namely, involving one to four N atoms of HMTA in coordination [13–34]. However, previous studies were mainly limited in using low coordination metal ion Ag(I) as spacers to connect HMAT [13-24], or using high coordination metal ions, such as Cd(II), Mn(II), as spacers to connect HMTA [25–31]. HMTA-based coordination polymers containing complex multidentate organic anions and high coordination metal ions remain rather rare [32-

34]. Here we focus on some metal ions full a shortage in previous studies. In between these ions which are characterized by their ability to form highly coordinated building. A deliberate investigation of new complexes prepared is the first aim in this study. Some special complexes were chosen for biological investigation. In which the complexes of methenamine are widely distributed in different application fields in betweens the biological activity.

2. Experimental

All chemicals used were analytical grade and were used without further purification.

2.1. The synthesis of some HMTA complexes

Ag(I), Cd(II), Hg(II), Cu(II), Ce(III), Sm(III) and La(III) complexes are prepared by adding a saturated aqueous solution of the respective metal salt to an ethanolic solution of HMTA by a molar ratio of 1:4, respectively. The product obtained were filtered, washed with ethanol and dried under vacuum at room temperature.

2.1.1. Sn (IV) – HMTA complex:

9 mmol (1.260 g) methenamine in methylenechloride (50 ml), was added drop wise with constant stirring to a freshly prepared solution of 3 mmol (0.7818 g) tin (IV) tetrachloride by a molar ratio 3 : 1, respectively. The resulting clear solution was left for 12 hrs. at room temperature with continuous stirring; the white precipitated was then filtered out, and washed several times and dried under vacuum over P_2O_5.

2.1.2. Sn (II) – HMTA complex:

The Sn(II) – HMTA complex was prepared by the addition of 0.896 g (4 mmol) of $SnCl_2.2H_2O$ to 1.12 g (8 mmol) of HMTA, both of them were dissolved in 50 ml ethanol. The reaction mixture was left for 8 hrs. with continuous stirring at room temperature. The white cream precipitated complex was then filtered out, washed several times with minimum ethylalchol and then dried under vacuum over P_2O_5.

2.1.3. Sb (III) and BiO (I) HMTA complexes:

Similar procedures were operated to prepare the two complexes. The antimony (III) trichloride and bismuth oxynitrate are reacted with HMTA in methanol as a solvent with a metal : ligand ratio by 1 : 3 at room temperature for about 8 – 10 hrs.

2.2. The Biological studies

The antimicrobial activity was applied by diffusion disc method. A filter paper sterilized disc saturated with measured quantity of the sample is placed on plate containing solid bacterial medium (nutrient agar broth) or fungal medium (Dox s medium) which has been heavily seeded with the spore suspension of the tested organism according to the method of Barry [35]. After inoculation, the diameter of the clear zone of inhibition surrounding the sample is taken as a measure of the inhibitory power of the sample against the particular test organism. The antibacterial activities of some investigated compounds were tested against Escherichia Coli and Staphylococcus Aureus as well as some kinds of fungi; Aspergillus Flavus and Candida Albicans. The complexes, the free HMTA and the pure solvent (DMSO) were tested with the antibacterial and antifungal investigation at the same time.

2.3. Physical and Instrumentation

Carbon, hydrogen and nitrogen contents were determined using a Perkin-Elmer CHN 2400 in the Micro-analytical Unit at the Faculty of Science, Cairo University, Egypt. The percentage of tin cations was determined using atomic absorption method. An atomic absorption spectrometer PYE – UNICAM SP 1900 fitted with a tin lamp was used for this purpose. The percentage of tin(IV) and tin (II) were also determined gravimetrically for conformation by transforming the product into the corresponding metal for tin (IV) and metal oxide for tin (II), while the antimony and bismuth contents are also determined as metals. The lanthanides were determined by complexometric titration using EDTA by xylenol orange [36]. The obtained analytical data are summarized in Table 1. FT IR spectra were investigated in the range 4000 – 400 cm^{-1} using a Gensis II FT IR spectrophotometer and samples were prepared as KBr discs. ^{1}HNMR spectra were recorded on a Varian Gemini 200 MHZ, at room temperature using dimethylsulphoxide as a solvent. Thermal studies of the prepared complexes were measured using a Shimadzu TGA -50H. The samples were heated in platinum crucible in a statistic nitrogen atmosphere to 600 ^{o}C at a heating rate 10 ^{o}C min^{-1}. The biological studies were carried out in Micro-Analytical Center, Faculty of Science, Cairo University, Egypt.

3. Results and Discussion

Methenamine reacts with, Ag(I), Cd(II), Hg(II), Cu(II), Sn(II), Sn(IV), Sb(III), Bi(III), Ce(III), Sm(III) and La(III) ions in non aqueous medium to form the obtained HMTA complexes. The physical and analytical data of the complexes are summarized in Table 1. The complexes are thermal stable in air and soluble in common organic solvents like DMSO. All the prepared complexes are non colored (white / white cream color) except for copper(II) complex. The colorless appearance observed for the isolated complexes devoted us to excluding the UV/ Vis study due to there is no significant bands characterized the complex geometry. So, the geometry proposed here referring to the most stable one for each metal ion, as well as the excepted attachment with the corresponding ligand and their conjugated anions (Fig. 1). In order to verify the presence of chloride is coordinated or ionic forms, the complex solution was tested with an aqueous $AgNO_3$ solution.

3.1. Spectroscopic Studies

3.1.1. IR Spectral Analysis

The characteristic spectral bands and their assignments for the isolated complexes in comparing with their relative ligand are presented in Table 2. The compounds are scanned over the range 4000 – 400 cm^{-1} which offer information regarding the coordination mode in the complexes. HMTA is a potentially tetradentate ligand. It may display different mode as a mono -, bi- , tri – or tetradentate. Framework molecular models show that it is more likely to act as monodentate ligand. This is through only one nitrogen atom from the four towards mononucleosis central atom or multidentate bridging ligand towards multi central atoms [37]. The fundamental bands in the ligand spectrum at 1250 and 1000 cm^{-1} are assigned to υC-N vibrations and split into doublets in all the complexes. This splitting elucidates the participation of some donor atoms in between the four for the same complex nucleolus. The IR spectra of

$[Cu_3(NO_3)_6(HMTA).3(H_2O)]$,
$[Ag(NO_3)(HMTA).2(H_2O)]$, $[CdCl_2(HMTA).(H_2O)]$ and $[Hg(NO_3)_2(HMTA).H_2O]H_2O$ complexes (Fig. 2, some examples) display a splitting in υC-N bands at $\approx$ 1250 cm^{-1} and $\approx$ 980 cm^{-1}. This is due to the differentiate behavior of the donor atoms and the non coordination of one or more in betweens. The minor splitting formed closely spaced doublets or triplets. The IR spectra associated with coordinated HMTA in the complexes reported here are almost super imposable on the IR spectrum of the uncoordinated ligand. This may be attributed to the fact that the chair configuration of the uncoordinated HMTA is retained in all these complexes [38]. The coordinated nitrate groups are terminally monodentate bonded towards Ag(I) and Hg(II) complexes and bidentated in multinuclear Cu(II) complex. This is through the appearance of new bands for υ_{as} and υ_s NO$_3$ by150 cm^{-1} difference, which may assigned for monodentate and 50 cm^{-1} difference for bidentate nature. The supplementary coordinating ligand (H$_2$O) was proposed based on the presence of new bands at lower frequency region (600 - 800 cm^{-1}) for δ_r and δ_w H$_2$O and over 3400 cm^{-1} for υOH, as well as the other supporting bands for υM-N and υM-OH$_2$. The IR spectra of $[SnCl_2(HMTA)_2]2H_2O$, $[SnCl_4(HMTA)_2]2H_2O$, $[SbCl_3(HMTA)_2]3H_2O$ and $[BiO(NO_3)(HMTA)_2.H_2O]$ $3H_2O$ as heavy metal complexes. These complexes were investigated concerning the same bands (υC-N). A band appeared at $\approx$ 1250 cm^{-1} and $\approx$ 1012 cm^{-1}, concerning 1012 cm^{-1} band displays a lower shift than the ligand. The lower appearance supports the participation of nitrogen atom

in coordination with the central atoms or with the hydrated water molecules through H- Bonding. The latter proposal is strongly supported through the relative thermal stability of these complexes during the TG investigation. The broad band in the range around 3500 cm^{-1} as well as new bands at the region $\approx$ 690 – 820 cm^{-1} for υOH, δr and δw, respectively. The rocking vibration associated to the CH$_2$ of HMTA is observed at 840 and 808 cm^{-1}, while the corresponding vibration of its complexes is observed as a strong absorption and found as group of bands lying in the 986 – 798 cm^{-1} region. The presence of these collected bands in the complexes under study, suggests that HMTA coordinates through its some donor atoms [39-42]. Finally other new bands appeared in all spectra at 499, 499, 510 and 515 cm^{-1} for Sn(II), Sn(IV), Sb(III) and BiO(I) complexes attributed to υM-N vibration. The IR spectra of $[CeCl_3(HMTA)_3]3H_2O$, $[SmCl_3(HMTA)_3]$ and $[La(NO_3)_3(HMTA)_3]3H_2O$ as inner transition metal complexes are investigated in comparing with the ligand spectrum. The significant υC-N bands appeared at $\approx$ 1250 and 980 cm^{-1} also reflects the presence of different behavior concerning the donor atoms. One or more in between donors may be coordinated towards the central metal ions the others may be non coordination or H – Bonded with hydrated water molecules. This proposal was confirmed through thermal analysis. The rocking vibration bands of CH$_2$ are also suffered shift ($\approx$ 560 - 790 cm^{-1}) due to the coordination of its neighboring atoms. Also, the appearance of new bands at $\approx$ 510 cm^{-1} in the complexes spectra are expected for υM-N band.
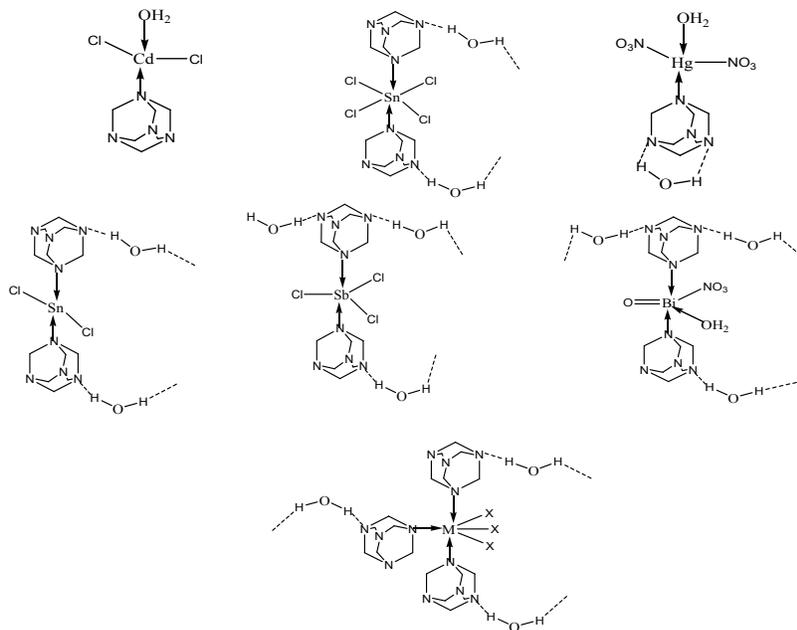
Fig. 1: The proposed structural formulae for most isolated complexes where as: M = Ce (X = Cl) or La (X = NO$_3$)

3.1.2. ^{1}HNMR Spectra

The ^{1}HNMR spectra of $[SnCl_2(HMTA)_2]2H_2O$ and $[BiO(NO_3)(HMTA)_2.H_2O]3H_2O$ complexes in DMSO $-d_6$ were carried out. Their spectra display whatever difference in comparing with their free ligand spectrum (standard spectrum), a shifted in $-CH_2-$ groups peaks to downfield (range from δ 4.41 to δ 5.11ppm for Sn (II) complex and from δ 4.25 to δ 5.08 ppm for Bi (III) complex) in comparing with the free HMTA ligand. Also, according to the ^{1}HNMR spectral data for $[SnCl_2(HMTA)_2]2H_2O$; δ = 3.45 [H , H_2O] and for $[BiO(NO_3)(HMTA)_2.H_2O]$ $3H_2O$ complex ; δ = 3.38 ,3.47 [H , H_2O] which not found in the spectrum of free HMTA compound , indicate the presence of water molecules in the two complexes. However, the presence of two peaks for H_2O in the Bi (III) complex may indicate that the water molecules found as coordinated lattice. The little difference proposed the presence of lattice molecules inside the coordination sphere through H – Bonding as previously proposed since these data are in agreement with the infrared and thermal analysis.

3.1.3. X – Ray diffraction study

X – Ray powder diffraction of the ligand and some of its complexes were done. The XRD of free ligand reflects its relative amorphous nature (Fig. 3) but the other investigated complexes (Hg(II), Ag(I), Sn(II) and BiO(I)) reveal a highly amorphous nature for the isolated solid complexes. This devoted us to exclude the idea of trying to isolate a single crystal from such complexes. This is may be due to the complexes are heavily hydrated through a strong physical bond with coordinated ligand which may deform crystalline structure in all isolated complexes.

3.2. Thermal analysis aspects

The correlations between the different decomposition steps of the complexes with the corresponding weight losses are reported in Table 3. All the new complexes prepared are thermally investigated. The TG and DTG curves of some complexes are shown in Figure 4. The thermogravimetric analysis is an essential for supporting the presence of solvent molecules coordinated with central atoms or in crystal lattice. The TG curves of multi nuclear $[Cu_3(NO_3)_6(HMTA).3H_2O]$ complex was degraded firstly at a high temperature (midpoint 234.2˚C) by a mass loss 33.83 (Calcd. 33.85 %) for the decomposition of $3H_2O + HMTA + NO_2 + 0.5O_2$. The final residue by 66.17 (Calcd. 66.15%) as a major part of a complex $[2Cu(NO_3)_2 + CuO + NO_2]$. The TG of $[Ag(NO_3)(HMTA). 2H_2O]$ complex displays two degradation stages ended at $\approx$ 550 ˚C. The first stage mid point at 226.25˚C may be for a decomposition of $2H_2O + NO_2 + CO+ N_2 + 6H_2$ by loss 50.7 (Calcd. 51.48%) weights. The second stage mid point at

458.89˚C may be corresponding to the removal of 3C atoms oxidized to their oxides by 10.51 (Calcd. 10.41%) weight losses. The final residue is AgC + C by weight percentage of 38.78(Calcd. 38.11%). The TG of $[CdCl_2(HMTA).H_2O]$ complex displays four degradation stages ended at $\approx$ 600 ˚C. The first stage mid point at 107.05˚C by 5.07 (Calcd. 5.27%) weight losses for the decomposition of H_2O coordinated with central atom. The following steps conclude the gradual decomposition of the coordinated ligand. The final residue at 600˚C by 10.02 (Calcd.10.55%) weights may be for the removal of 3C atoms. The TG curve of $[Hg(NO_3)_2(HMTA)(H_2O)]H_2O$ starts degradation at temperature mid point 88.75˚C may be assigned to the removal of $2(H_2O) + L + 2NO_2 + O_2$ by 60.09 (Calcd. 59.94%) weight losses. The residue recorded at 246.6˚C assigned for Hg by 39.89 (Calcd. 40.05%) weights. The TG curve of $[SnCl_4(HMTA)_2]2H_2O$ complex starting the decomposition at first stage mid point at 140˚C corresponding to the removal of hydrated molecules bonded through H – Bonding inside the coordination sphere by 6.2 (Calcd. 6.24%) weight percentage. The final residue assigned to Sn atom by 20.19(Calcd. 20.58%). The TG curve of $[SnCl_2(HMTA)_2]2H_2O$ complex is starting the decomposition at the mid point temperature 240˚C may be corresponding to the removal of $2H_2O + Cl_2 + 2HMTA$ by 76.32(Calcd. 76.54%) weight losses and the residual part assigned for Sn by 23.68(Calcd. 23.36%). The TG curve of $[SbCl_3(HMTA)_2]3H_2O$ complex displays a decomposition step by a major fragments weights by 78.81(Calcd. 78.89%) and the residual part includes the Sb only by 21.19(Calcd. 21.103%). The TG curve of $[BiO(NO_3)(HMTA)_2.H_2O]$ $3H_2O$ complex displays two degradation stages starting firstly at temperature mid point 150˚C which corresponding to the removal of hydrated water molecules by 8.51 (Calcd. 8.45%) weight loss. The second decomposition stage at mid point temperature 305˚C is corresponding to the removal of coordinated water molecule beside the ligands completely by 46.6 (Calcd. 46.67%) weight losses. The final residue may be corresponding to $BiO(NO_3)$. The TG curve of $[CeCl_3(HMTA)_3.3H_2O]$ complex displays two degradation stages starting at $\approx$ 300˚C (mid point) may be corresponding to the removal of 1.5 $Cl_2 + 3H_2O$ by 22.00 (Calcd. 22.24%). The second stage at 513˚C may be corresponding to the removal of $2HMTA + C_6H_{12}N$ by 51.18(Calcd. 52.49%). The final residue may be for CeN_3 by 26.8(Calcd. 25.26%). The TG curve of $[SmCl_3(HMTA)_3]$ complex displays two degradation stages starting at 270˚C (mid point) may be corresponding to the removal of $1.5Cl_2$ +HMTA by 36.1 (Calcd. 36.4%). The second stage mid point at $\approx$ 430˚C by 40.0(Calcd. 41.39%) may be corresponding to removal of 2HMTA molecules. The residual part is

representing to Sm by 23.89(Calcd. 22.21%). The TG curve of $[La(NO_3)_3(HMTA)_3]3H_2O$ complex displays three degradation stages. The first stage mid point at 95°C by 2.19 (Calcd. 2.25%) weight losses assigned for the removal of hydrated H_2O molecule. The second stage at 135°C is corresponding to the removal of $2H_2O$ by 4.59(Calcd. 4.50%). The third stage at 321°C by 75.29(Calcd. 75.8%) may be corresponding to the removal of $3HMTA + 3NO_2 + 1.5O_2$. The residual part represents La by 17.93(Calcd. 17.37%). All the data abstracted from the thermal study supporting the proposal of presence of hydrated and coordinated water molecules. Also, the trend of decomposition in relatively higher temperature supports the interaction of solvent molecules inside the coordination sphere through the H- Bonding with the active donor atoms in the ligand as the same as coordinated molecules. Such by the relative thermal stability recorded for most complexes. Most complexes display the same trend in degradation by showing 1 to 2 degradation steps and corresponding to expel of all surrounds of central metal atoms in most investigated complexes except some of them which containing other coherent with the central atoms. This may be due to the recording of residual at relatively lower temperature as well as the strength of bonds coherently attached with metal atoms. This H-Bonding stabilizing the complexes towards the thermal decomposition at relatively higher temperature.

3.3. Thermal decomposition kinetics

Recently, there has been increasing interest in determining the rate-dependent parameters of solid-state non-isothermal decomposition reactions by analysis of TG curves [43,44]. The kinetic analysis parameters such as activation energy (E*), enthalpy of activation (ΔH^*), entropy of activation (ΔS^*), free energy change of decomposition (ΔG^*) were evaluated graphically by employing the Coats–Redfern relation [45] for Cu(II), Ag(I), Cd(II) and Hg(II) complexes (Table 4).

$$\ln\left[\frac{1-(1-\alpha)^{1-n}}{(1-n)T^2}\right] = \frac{M}{T} + B \quad \text{for n} \neq 1 \quad (1)$$

$$\ln\left[\frac{-\ln(1-\alpha)}{T^2}\right] = \frac{M}{T} + B \quad \text{for n =1} \quad (2)$$

Where $M=-E/R$ and $B = \ln AR/\Phi E$; E, R, A, and Φ are the heat of activation, the universal gas constant, pre-exponential factor and heating rate, respectively. The correlation coefficient, r, was computed using the least square method for different values of n, by plotting the left-hand side of Eqs. (1) or (2) versus $1000/T$ (Fig. 5). A plot of left hand side of Eq. (1) against $1/T$ gives a slope from which E* was calculated and A (Arrhenius constant) was determined from the intercept. From relevant data, linearization

plots confirm first order kinetics. It has been found that E* values for complexes > ligand. The entropy of activation (ΔS^*) and the free energy change of activation (ΔG^*) were calculated using Eqs. (3) and (4):

$$\Delta S^* (JK^{-1} mol^{-1}) = R [\ln(Ah/kT)-1] \quad (3)$$

$$\Delta G^*(J mol^{-1}) = \Delta H^* - T\Delta S^* \quad (4)$$

Where; k and h are the Boltzman and Plank constants, respectively. The calculated values of ΔE^*, A, ΔS^* and ΔG^* for the decomposition steps of the complexes are given in Table 4. According to the kinetic data obtained from the TG curves, all the complexes have negative entropy, which indicates that the complexes are formed spontaneously. The negative entropy also indicates a more ordered.

3.4. Biological Studies

From the antimicrobial profile (Table 5), Hg-HMTA displays a significant inhibitory effect on the growth of tested fungal and bacterial species followed by Cd-HMTA and Ag- HMTA, regarding to the standard antibacterial and antifungal agents. A relative inhibitory effect on the growth of tested bacterial and fungal isolates was observed by Ag-HMTA. Unlike, the slightly antibacterial activity of Cu has relatively no antifungal activity. The plausible antifungal and antibacterial activities by Hg-HMTA and Cd – HMTA complexes may be attributed to the toxicity of Hg and Cd ions on plasma membrane functions, by interference with the ATP binding domains or amino acid transporter channels, causing a negative effect on some metabolic pathways, especially metalloproteinase dependent. According to Overtone's concept [46] of cell permeability, the lipid membrane that surrounds the cell favors the passage of only lipid soluble materials due to the liposolubility is an important factor that controls antimicrobial activity. On chelation, the polarity of the metal ion is reduced to a great extent due to the overlap of the ligand orbital and partial sharing of the positive charge of the metal ion with donor groups. The reduction in positive charge of the central metal ion is greater for oxidation states I and II than the oxidation state III, so here we focus on some special complexes which may serve based on the previous concepts. The increased lipophilicity enhances the penetration of the complexes into lipid membranes and blocking the metal binding sites on the enzymes of the microorganism. Also, however the metal salts alone may exhibit a higher activity than the complexes but cannot be used as antibacterial agents because of their toxicity and the probability of binding to the free ligands presented in the biological systems such as the nitrogen bases of nucleic acid and proteins.

Table 1: Analytical and Physical data for HMTA metal complexes

Compound Empirical formula (M. Wt.)	Color (geometry)	Elemental analysis (%) Calcd. (Found)				
		C	H	N	M	Cl
1) [Cu$_3$ (NO$_3$)$_6$ (C$_6$H$_{12}$N$_4$) 3H$_2$O] (756.89)	Blue (distorted octahedral)	9.52(9.60)	2.39(2.35)	-----	25.2(25.1)	------
2) [Ag (NO$_3$) (C$_6$H$_{12}$N$_4$). 2H$_2$O] (346.09)	Buff (tetrahedral)	20.82(20.80)	4.66(4.60)	20.24(20.27)	31.17(31.14)	------
3) [Cd Cl$_2$ (C$_6$H$_{12}$N$_4$) H$_2$O] (341.52)	White (Tetrahedral)	21.1(21.20)	4.13(4.14)	16.40(16.50)	32.91(32.87)	20.76(20.65)
4) [Hg (NO$_3$)$_2$(C$_6$H$_{12}$N$_4$) (H$_2$O)] (H$_2$O)(500.82)	White (Tetrahedral)	14.39(14.40)	3.22(3.30)	16.78(16.60)	40.05(40.15)	----
5) [Sn Cl$_4$ (C$_6$H$_{12}$N$_4$)$_2$]2H$_2$O (576.93)	White (Octahedral)	24.98(24.96)	4.89(4.87)	19.42(19.40)	20.58(20.57)	24.58(24.57)
6) [SnCl$_2$(C$_6$H$_{12}$N$_4$)$_2$]2H$_2$O (506.02)	White (Tetrahedral)	28.48(28.45)	5.58(5.57)	22.14(22.19)	23.46(23.44)	14.01(14.00)
7) [Sb Cl$_3$(C$_6$H$_{12}$N$_4$)$_2$]3H$_2$O (562.53)	White (Trigonal bipyramidal)	25.62(25.60)	5.37(5.36)	19.92(19.87)	21.64(21.64)	18.91(18.90)
8) [BiO(NO$_3$)(C$_6$H$_{12}$N$_4$)$_2$(H$_2$O)] 3H$_2$O(639.42)	Whit (Trigonal bipyramidal)	22.54(22.53)	5.04(5.10)	19.71(19.65)	32.68(32.66)	-----
9) [Ce Cl$_3$(C$_6$H$_{12}$N$_4$)$_3$]3H$_2$O (721.09)	White (Octahedral)	29.98(30.10)	5.87(5.88)	23.31(23.32)	19.43(19.42)	14.75(14.76)
10) [SmCl$_3$(C$_6$H$_{12}$N$_4$)$_3$] (677.29)	White (Octahedral)	31.92(31.88)	5.36(5.34)	24.82(24.80)	22.20(22.20)	15.70(15.60)
11) [La(NO$_3$)$_3$(C$_6$H$_{12}$N$_4$)$_3$]3H$_2$O (799.53)	White (Octahedral)	27.04(27.03)	5.29(5.28)	----	17.37(17.38)	-----

Table 2: Assignments of the IR Spectral bands (cm^{-1}) of HMTA and its metal complexes

Compound	υ (C-N)	υ(H$_2$O)	δ_r(H$_2$O)	δ_w(H$_2$O)	υ(NO$_3$)	ν_{M-N}	ν_{M-O}
1) [C$_6$H$_{12}$N$_4$]	1250	1000	---	---	---	----	----	---
2) [Cu$_3$ (NO$_3$)$_6$ (C$_6$H$_{12}$N$_4$) 3H$_2$O]	1100	900	3550	800	700	1400 1350	470	550
3) [Ag (NO$_3$) (C$_6$H$_{12}$N$_4$). 2H$_2$O]	1000	980	3500	800	650	1450 1300	500	520
4) [Cd Cl$_2$ (C$_6$H$_{12}$N$_4$) H$_2$O]	1250	1000 980	3500	800	650	----	500	520
5) [Hg (NO$_3$)$_2$(C$_6$H$_{12}$N$_4$) (H$_2$O)] (H$_2$O)	1050	1000	3500	800	700	1450 1350	500	550
6) [Sn Cl$_4$ (C$_6$H$_{12}$N$_4$) $_2$]2H$_2$O	1250	1018	3480	818	798	---	499	---
7) [SnCl$_2$(C$_6$H$_{12}$N$_4$)$_2$]2H$_2$O	1253	1012	3475	818	693	---	499	----
8) [Sb Cl$_3$(C$_6$H$_{12}$N$_4$)$_2$]3H$_2$O	1269	1018	3433	800	690	---	510	----
9) [BiO(NO$_3$)(C$_6$H$_{12}$N$_4$)$_2$(H$_2$O)]3H$_2$O	1264	1018	3422	818	745	1468 1295	515	-----
10) [Ce Cl$_3$(C$_6$H$_{12}$N$_4$)$_3$]3H$_2$O	1259	1012	3564	818	792	----	520	----
11) [SmCl$_3$(C$_6$H$_{12}$N$_4$)$_3$]	1250	1012	3427	800	712	----	525	----
12) [La(NO$_3$)$_3$(C$_6$H$_{12}$N$_4$)$_3$]3H$_2$O	1243	1012	3532	818	750	1468 1290	509	----

Table 3: Thermogravimetric data of the investigated complexes

Complex	Steps	DTG peak (°C)	Decomposed assignments	Weight loss Found (Calcd. %)
(2)	1st	234.22	$-NO_3 + L + 3H_2O$	33.83 (33.85)
	residue		$-2[Cu(NO_3)_2] + Cu + NO_2 + 0.5O_2$	66.17 (66.15)
(3)	1st	226.25	$-2H_2O + NO_2 + 0.5O_2 + 2N_2 + 6H_2 + C$	50.70 (51.48)
	2nd	458.89	$-3C$	10.51 (15.41)
	residue		$Ag + 2C$	38.78 (38.11)
(4)	1st	107.05	$-H_2O$	5.07 (5.27)
	2nd	208.93	$-Cl_2 + N_2$	28.29 (28.96)
	3rd	241.4	$-C + 3H_2$	5.56 (5.28)
	4th	329.13	$-Cd + 2C + 3H_2 + N_2$	51.06 (49.92)
	residue		$3C$	10.02 (10.55)
(5)	1st	88.75	$-2H_2O + L + 2NO_2 + O_2$	60.09 (59.94)
	residue	246.6	Hg	39.89 (40.05)
(6)	1st	140	$-2H_2O$	6.20 (6.24)
	2nd	240	$-2L + 2Cl_2$	73.61 (73.18)
	residue		Sn	20.19 (20.58)
(7)	1st	240	$-2H_2O + 2L + 2Cl_2$	76.32(76.54)
	residue		Sn	23.68(23.36)
(8)	1st	270	$-3H_2O + 2L + 1.5Cl_2$	78.81(78.89)
	residue		Sb	21.19(21.103)
(9)	1st	150	$-3H_2O$	8.51(8.45)
	2nd	295	$-H_2O + 2L$	46.60(46.67)
	residue		$BiO(NO_3)$	44.89(44.88)
(10)	1st	307	$-1.5Cl_2 + 3H_2O$	22.00(22.24)
	2nd	513	$-3C_6H_{12}N + 2L +$	51.18(52.49)
	residue		CeN_3	16.81(25.26)
(11)	1st	272	$-1.5Cl_2$	36.10(36.40)
	2nd	433	$2L$	40.00(41.39)
	residue		Sm	23.89(22.21)

Table 4: Kinetic parameters using the Coats – Red fern (CR)operated for the HMTA complexes

Complex	Step	Method	Kinetic Parameters					
			E ($Jmol^{-1}$)	A (S^{-1})	ΔS ($Jmol^{-1}K^{-1}$)	ΔH ($Jmol^{-1}$)	ΔG ($Jmol^{-1}$)	r
(2)	1st	CR	1.02×10^5	1.5×10^2	-2.08×10^2	9.76×10^4	2.03×10^5	0.9746
(3)	1st	CR	4.81×10^5	7.11×10^2	-1.9×10^2	4.77×10^5	5.74×10^5	0.9859
	2nd	CR	2.85×10^5	4.22×10^2	-2.02×10^2	2.79×10^5	4.27×10^5	0.9402
(4)	1st	CR	1.22×10^5	1.80×10^2	-2.04×10^2	1.19×10^5	1.96×10^5	0.9177
	2nd	CR	1.43×10^5	2.11×10^2	-2.05×10^2	1.39×10^5	2.44×10^5	0.9594
	3rd	CR	1.84×10^5	2.72×10^2	-2.07×10^2	1.77×10^5	3.53×10^5	0.9935
(5)	1st	CR	1.17×10^5	1.73×10^2	-2.06×10^2	1.13×10^5	2.11×10^5	0.9941
	2nd	CR	1.16×10^5	1.71×10^2	-2.07×10^2	1.12×10^5	2.20×10^5	0.9750

Table 5 :The inhibition zone values of bacteria and fungi for the ligand and its metal complexes

Compound	Escherichia coli (G⁻)	Staphylococcus Aureus (G⁺)	Aspergillus flavus (Fungus)	Candida albican (Fungus)
DMSO	0.0	0.0	0.0	0.0
Tetracycline	32	26	--	--
Amphotricin B	--	--	17	20
[$Cu_3 (NO_3)_6 (C_6H_{12}N_4)$ $3H_2O$]	13	14	0.0	13
[$Ag (NO_3) (C_6H_{12}N_4)$. $2H_2O$]	25	24	13	17
[$Cd Cl_2 (C_6H_{12}N_4) H_2O$]	31	35	18	24
[$Hg(NO_3)_2(C_6H_{12}N_4) (H_2O)$] ($H_2O$)	35	36	23	29
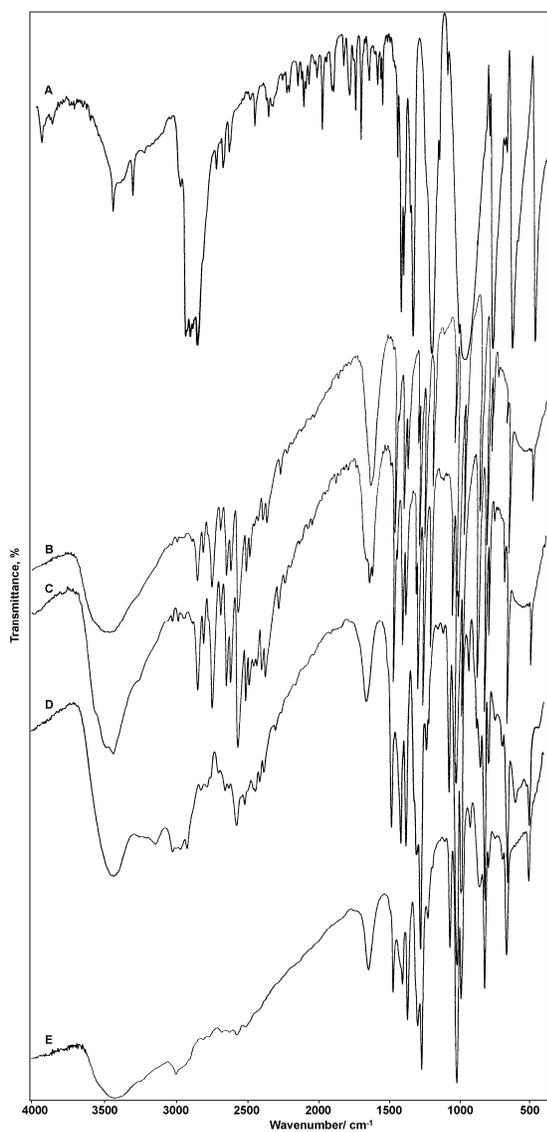
Fig. 2: Infrared spectra of (A) Free HMTA, (B) Sn(IV)-HMTA, (C) Sn(II)-HMTA, (D) Sb(III)-HMTA and (E) Bi(III)-HMTA complexes.
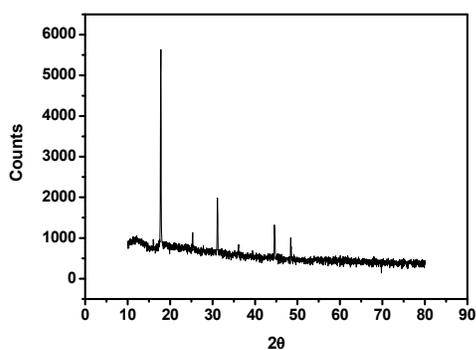
Fig. 3: XRD of HMTA in free State
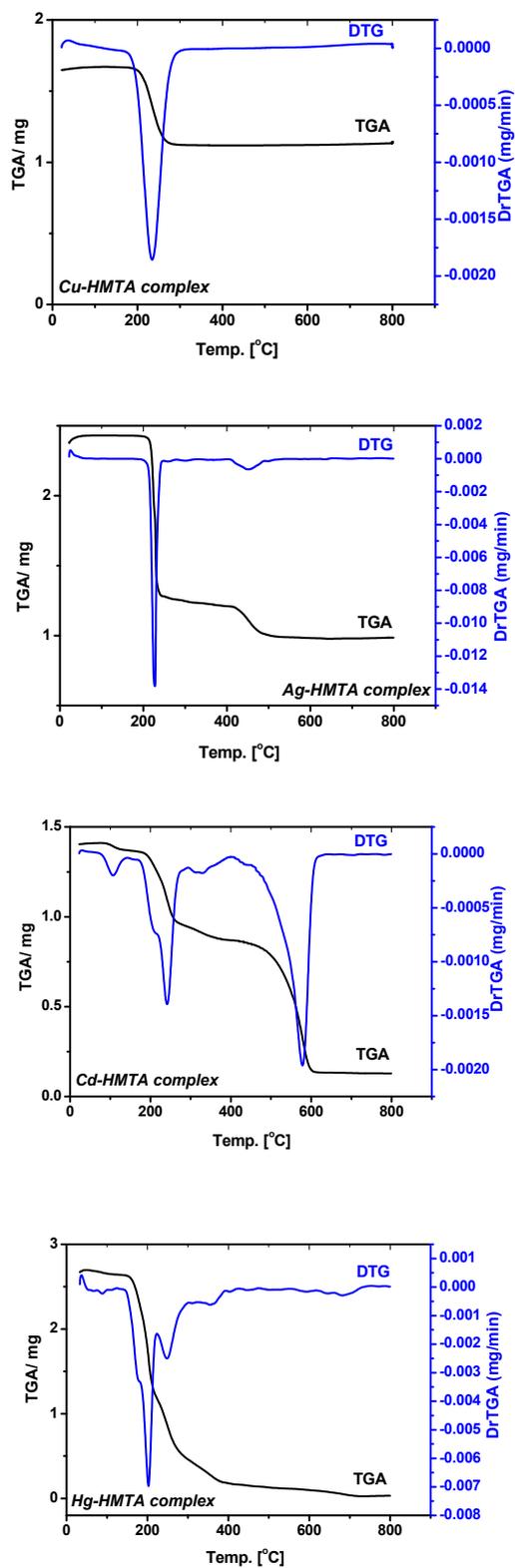
Fig. 4: Thermogravimetric analysis TG and DTG of HMTA complexes.
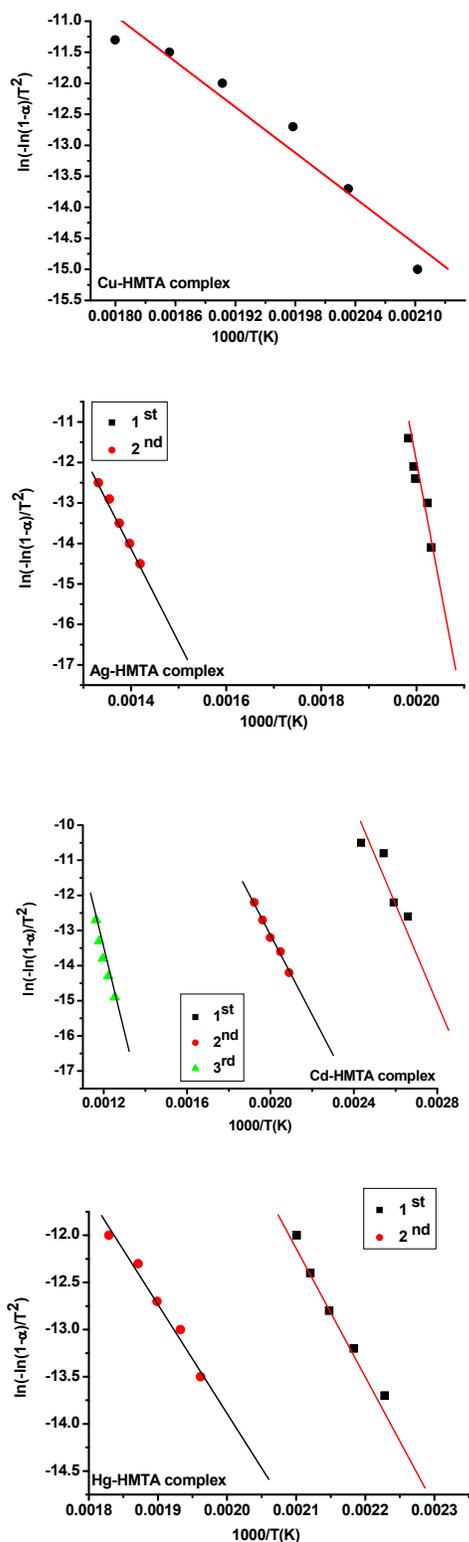
Fig. 5: Coats–Redfern curves of Cu(II), Ag(I), Cd(II) and Hg(II) HMTA complexes.

Corresponding author
Soha F. Mohammed[a]
Chemistry Department, Faculty of Science, Zagazig University, Zagazig Egypt.
sofahim@yahoo.com

References

1. Ezuhara T., K. Endo and Y. Aoyama,(1999). Helical Coordination Polymers from Achiral Components in Crystals. Homochiral Crystallization, Homochiral Helix Winding in the Solid State, and Chirality Control by Seeding, J. Am. Chem. Soc. **121**, 3279.

2. Kondo M., T. Yoshitomi, K. Seki, H. Matsuzaka and S. Kitagawa, (1997). Three-Dimensional Framework with Channeling Cavities for Small Molecules: $\{[M_2(4, 4'\text{-bpy})_3(NO_3)_{4]}\cdot xH_2O\}n$ (M = Co, Ni, Zn) , Angew. Chem. Int. Ed. Engl. **36**, 1725.

3. Reineke T.M., M. Eddaoudi, M. O'Keefe and O.M. Yaghi, (1999). A Microporous Lanthanide–Organic Framework, A ngew. Chem. Int. Ed. Engl. **38**, 2590;

4. Inoue K., T. Hayamizu, H. Iwamura, D. Hashizume and Y. Ohashi, (1996). Assemblage and Alignment of the Spins of the Organic Trinitroxide Radical with a Quartet Ground State by Means of Complexation with Magnetic Metal Ions. A Molecule-Based Magnet with Three-Dimensional Structure and High TCof 46 K, J. Am. Chem. Soc. **118**, 1803.

5. Fujita M., Y.J. Kwon, S. Washizu and K. Ogura, (1994). Preparation, Clathration Ability, and Catalysis of a Two-Dimensional Square Network Material Composed of Cadmium(II) and 4,4'-Bipyridine, J. Am. Chem. Soc. **116**, 1151.

6. Russell V.A., C.C. Evans, W. Li and M.D. Ward, (1997). Nanoporous Molecular Sandwiches: Pillared Two-Dimensional Hydrogen- Bonded Networks with Adjustable Porosity, Science **276**, 575.

7. Carlucci L., G. Ciani, D.M. Proserpio and A. Sironi, (1995). Novel Networks of Unusually Coordinated Silver(I) Cations: The Wafer-Like Structure of $[Ag(pyz)_2][Ag_2(pyz)_5]$ $(PF_6)3\cdot 2G$ and the Simple Cubic Frame of $[Ag(pyz)_3](SbF_6)]$, Angew. Chem. Int. Ed. Engl. **34**, 1895.

8. Li H., M. Eddaoudi, M. O'Keeffe and O.M. Yaghi, (1999). Design and synthesis of an exceptionally stable and highly porous metal-organic framework , Nature **402**, 276.

9. Noro S.-i., S. Kitagawa, M. Kondo, K. Seki, (2000). A New, Methane Adsorbent, Porous Coordination Polymer $[\{CuSiF_6(4,4'\text{-}$

bipyridine)$_2$}n], Angew. Chem. Int. Ed. Engl. **39**, 2081.

10. Wang Q.M., G.C. Guo and T.C.W. Mak, (1999). A coordination polymer based on twofold interpenetrating three-dimensional four-connected nets of 42638 topology, [CuSCN(bpa)] [bpa = 1,2-bis(4-pyridyl) ethane], Chem. Commun., 1849.

11. Ponomarova V.V., V.V. Komarchuk, I. Boldog, A.N. Chernega, J. Sieler and K.V. Domasevitch, (2002). A coordination polymer based on twofold interpenetrating three-dimensional four-connected nets of 42638 topology, [CuSCN(bpa)] [bpa = 1,2-bis(4-pyridyl)ethane], Chem. Commun., 436.

12. Rather B., B. Moulton, R.D.B. Walsh and M.J. Zaworotko, (2002). A new supramolecular isomer of [Zn(nicotinate)$_2$]$_\mathbf{n}$: a novel $4^2.8^4$ network that is the result of self-assembly of 4-connected nodes, Chem. Commun., 694.

13. Carlucci,L. G. Ciani, D.M. Proserpio and A. Sironi, (1995). A Three-Dimensional, Three-Connected Cubic Network of the SrSi$_2$ Topological Type in Coordination Polymer Chemistry: [Ag(hmt)](PF$_6$).cntdot.H$_2$O (hmt = Hexamethylenetetraamine), J. Am. Chem. Soc. **117**, 12861.

14. Carlucci L., G. Ciani, D.W.V. Gudenberg, D.M. Proserpio and A. Sironi, (1997). Self-assembly of a three-dimensional network from two-dimensional layers via metallic spacers: the (3,4)-connected frame of [Ag$_3$(hmt)$_2$][ClO$_4$]$_3$·2H$_2$O (hmt= hexamethylenetetramine), Chem. Commun., 631.

15. Carlucci L., G. Ciani, D.M. Proserpio and A. Sironi, (1997). A Novel 3D Three-Connected Cubic Network Containing [Ag$_6$(hmt)$_6$]$^{6+}$Hexagonal Units (hmt = Hexamethylenetetramine), Inorg. Chem. **36**, 1736.

16. Carlucci L., G. Ciani, D.M. Proserpio and S. Rizzato, (2000). Structural Properties and Topological Diversity of Polymeric Ag(I)-hexamethylenetetramine Complexes: Self-Assembly of Three Novel Two-Dimensional Coordination Networks and Their Supramolecular Interactions, J. Solid State Chem. **152**, 211.

17. Tong M.L., S.L. Zheng and X.M. Chen, (1999) [Two- and three-dimensional non-interpenetrating open-networks self- assembled by μ4-hexamethylenetetramine (hmt). Syntheses and structures of [Ag2(μ4-hmt)(SO$_4$)(H$_2$O)]·4H$_2$O and [Ag$_2$ (μ$_4$-hmt)(μ-O$_2$CMe)]MeCO$_2$·4.5H$_2$O] Chem. Commun.; 561.

18. Zheng S.L., M.L. Tong, H.L. Zhu, Y. Fang and X.M. Chen, (2001). Syntheses and structures of three two-dimensional silver(I)–hexamethylenetetramine co-ordination polymers with new topological motifs, Chem. Soc., Dalton Trans., 2049.

19. Zheng S.L., M.L. Tong, X.L. Yu and X.M. Chen, (2001). Syntheses and structures of six chain-, ladder- and grid-like co-ordination polymers constructed from μ-hexamethylenetetramine and silver salts, J. Chem. Soc., Dalton Trans., 586.

20. Zheng S.L., M.L. Tong, R.W. Fu and X.M. Chen, (2001). Toward Designed Assembly of Microporous Coordination Networks Constructed from Silver(I)− Hexamethylene-tetramine Layers, Inorg. Chem. **40**, 3562.

21. Bu W.M., L. Ye and Y.G. Fan, (2000). Syntheses and structures of two- and three-dimensional coordination networks generated from silver complexes and hmt (hmt=hexamethylenetetramine), Inorg. Chem. Commun. **3**, 194.

22. Zheng S.L., M.L. Tong and X.M. Chen, (2002). Recent Progress in Construction of the Molecular Architectures Based on Ag(I)-Hexamethylenetetramine, Chin. J. Inorg. Chem. **18**, 17.

23. Zheng S.L., M.L. Tong and X.M. Chen, (2003). Silver(I)–hexamethylenetetramine molecular architectures: from self-assembly to designed assembly, Coord. Chem. Rev. **246**, 185.

24. Liu Q., X.Q. Sun, Y.Q. Zhu, B.L. Li, Z. Xu, H.B. Liu and K-B. Yu, (2001). Synthesis and crystal structure of [Ag$_2$(μ$_4$-hmt)(NO$_2$)$_2$]n. A two-dimensional network with square cavities self-assembled by hmt (hmt = Hexamethylenetetramine), Transition. Met. Chem. **26**, 369.

25. Liu Q., X.Q. Sun, J.-Z. Zou, Z. Xu and K.-B. Yu, (2002). A New Azide-Bridged Three-Dimensional Supramolecular Manganese(II) Compound: Synthesis, Crystal Structure and Magnetic Properties, J. Coord. Chem. **55**, 1021.

26. Liu Q., B.L. Li, X.Q. Sun, Z. Xu and K.B. Yu, (2001). Diaquabis(hexamethylenetetramine-N)-bis(isothiocyanato)manganese(II) tetraaquabis-(isothiocyanato)manganese(II) dehydrate, Acta. Cryst. Sect. E. E57, m151.

27. Liu Q., H.-T. Xi, X.-Q. Sun and J.-F. Zhu and Y. Kai-Bei, (2002). Synthesis and crystal structure of trans-diaquabis (hexamethylene tetramine-N)bis(isothiocyanato)cobalt(II) trans-

tetraaquabis(isothiocyanato)cobalt(II) dehydrate, Chin. J. Struct. Chem. **21**, 355.

28. Pan L., N.W. Zheng, Y.G. Wu, W.J. Zheng and X.T. Wu, (2000). A three-dimensional structure, four-connected network of the zeolite Li–A(BW) topological frame sustained by [Hg(hmt)1/2Br$_2$] units via secondary bonding, Inorg. Chim. Aata. **303**, 121.

29. Zheng Y., J. Li, M. Nishiura and T. Imamoto, (2000). Structural, spectral and thermal properties of a polymeric nickel(II) complex containing two-dimensional network, J. of Mol. Struct. **520,** 259.

30. T.C.W. Mak, (1982). Crystal structure of hexamethylenetetramine-cadmium iodide-water, Z. Kristallogr. **159**, 247.

31. Moulton B., J. Lu and M.J. Zaworotko, (2001). Periodic Tiling of Pentagons: The First Example of a Two-Dimensional (5_4^3)-net, J. Am. Chem. Soc. **123**, 9224.

32. Batten S.R., B.F. Hoskins and R. Robson, (1998). Synthesis and Rutilelike Structure of [Cd(tcm)(hmt)(H$_2$O)](tcm) (tcm= Tricyanomethanide, C(CN)$^{3-}$; hmt= Hexamethylenetetramine), Inorg. Chem. **37**, 3432.

33. Liu Q., B.L. Li, Z. Xu, X.Q. Sun and K-B. Yu, (2002). A novel three-dimensional coordination polymer [Cd$_2$(C$_3$H$_2$O$_4$)$_2$(H$_2$O)$_2$ (μ_2-hmt)]n(hmt = hexamethylenetetramine): synthesis and crystal structure, Transition. Met. Chem. **27**, 786.

34. Liu Q., B.L. Li, Z. Xu and K-B. Yu, (2003). Synthesis, Crystal Structure and Magnetic Property of [Mn2(mal)2(H2O)2(μ2-hmt)]n: A Novel Three-Dimensional Network Self-Assembled by hmt (hmt = Hexamethylene-tetramine and mal = Malonate), J. Coord. Chem. **56**, 771.

35. Barry A. L.: Procedures of testing antimicrobial agents in agar media. Antibiotics in Laboratory Medicine, Lorin, Williams Wilkins Co. Baltimore, USA, 1-23 (1980).

36. Busiew A. I., W. G. Tipcova and W. M. Ivanov, analytical Chemistry of Rare Elements, WNT Warsaw, Polish Translation, (1982).

37. Ahuja I. S., R. Singh and C. L. Yadava, (1980). Structural information on cobalt(II), nickel(II), copper(II), zinc(II), silver(I) and cadmium(II) nitrate complexes with hexamethylenetetramine from their magnetic moments, electronic and infrared spectra, J. of Mol. Struct. **68**, 333.

38. Finar I. L., Organic Chemistry, Vol. I, Longmans, London, (1973).

39. Konar S. ; P. S. Mukherjee; M. G. B. Drew ; J. Ribas and N. R. Chaudhuri , (2003). Syntheses of Two New 1D and 3D Networks of Cu(II) and Co(II) Using Malonate and Urotropine as Bridging Ligands: Crystal Structures and Magnetic Studies. Inorganic Chemistry **42(8),** 2545.

40. Dagur P. ;D.Chopra ; A.S.Prakash ; T. N. Guru Row and M. S.Hegde, (2003). Hexaaqua-nickel(II) dichromate bis(hexamethylenetetr-amine) monohydrate, Acta Crystallgraphica E 59(12) , m1129.

41. Zalewicz M., (1990). The synthesis and thermal decomposition of complex salts of lanthanide bromides with hexamethylene- tetramine, Thermochim. Acta **171**, 131.

42. Xue, F. and T.C.W. Mak, (1996). Supramolecular Framework Adducts Constructed of Hexamethylenetetramine, Aquated Alkali Metal Cationic Clusters, and Hexacyanoferrates(II/III), Struct. Chem. **7**, 253.

43. Singh B.K., R.K. Sharma and B.S. Garg, (2006). Kinetics and molecular modeling of biologically active glutathione complexes with lead(II) ions, J. Therm. Anal. Cal. **84**, 593.

44. Singh B.K., N. Bhojak, P. Misra and B.S. Garg, (2008). Copper(II) complexes with bioactive carboxyamide: Synthesis, characterization and biological activity, Spectrochim. Acta A **70**, 758.

45. Coats A.W. and J.P. Redfern, (1964). Kinetic Parameters from Thermogravimetric Data 68, Nature **201**, 68.

46. Raman N., J. Joseph, A. Senthil Kumara Velan1 and C. Pothiraj, (2006). Antifungal Activities of Biorelevant Complexes of Copper(II) with Biosensitive Macrocyclic Ligands, Mycobiology **34**, 214.

5/21/2012